First publ. in: Soft matter ; 23 (2010), 6. - pp. 5860-5863

Nanoparticle assembly by confinement in wrinkles: experiment and simulations

Alexandra Schweikart,[a] Andrea Fortini,[b] Alexander Wittemann,[a] Matthias Schmidt[bc] and Andreas Fery*[a]

DOI: 10.1039/c0sm00744g

We created hierarchically ordered structures of nanoparticles on smooth planar hydrophilic substrates by drying colloidal dispersions in confinement under macroscopic stamps with microscopically wrinkled surfaces. Experiments were carried out with model nanoparticle suspensions that possess high colloidal stability and monodispersity. The structures ranged from single parallel lines of particles to arrays of dense prismatic ridges. The type of observed structure could be controlled by the particle concentration in the initial dispersion. Confinement between two crossed stamps led to interconnected meshes of particles. The precise morphology could be predicted in all cases by Monte Carlo computer simulations of confined hard spheres. Our findings open up possibilities for versatile nanoparticle assembly on surfaces.

Ordered arrays of nanoparticles form excellent candidates for components of future optical, electronic and magnetic devices,[1,2] for creating biomimetic surfaces,[3] and for exploiting their plasmonic properties.[4,5] Control of the precise placement of the particles on a solid surface is a prerequisite for the technological use of the unique, size-specific properties of the nanoparticles.

Primary strategies for controlling the spatial arrangement of much larger, micron-sized colloids include the deposition of particle monolayers on chemically or topographically structured substrates,[6–9] epitaxial growth[10,11] and confinement.[12,13] Structures with periodicities comparable to the wavelength of visible light are interesting as these enable one to make use of their optical band structure. In particular, linear assemblies, such as particle wires,[14,15] possess high potential for photonic applications. Nevertheless, both structuring on the smaller (nano) scale, as well as obtaining macroscopic coverage of the substrate is desirable in attempting to bridge all length-scales. Both physical[6,9] and chemical[7,8] properties of surfaces can be used in order to create templates for the adsorption of particles. Topographic templates can be produced using photolithographic[1,2] and soft lithographic[16–18] techniques or, alternatively, by controlled wrinkling.[19,20] Wrinkles with well-defined wavelength form if an elastomeric substrate that is coated with a thin, hard layer is exposed to a lateral compressive strain.[21] Significant benefits of this approach are its low cost and the simplicity of scaling up the size of the structured substrate to macroscopic dimensions.

[a]*Physikalische Chemie I & II, Universität Bayreuth, Universitätsstraße 30, D-95440 Bayreuth, Germany. E-mail: andreas.fery@uni-bayreuth.de*
[b]*Theoretische Physik II, Physikalisches Institut, Universität Bayreuth, Universitätsstraße 30, D-95440 Bayreuth, Germany*
[c]*H. H. Wills Physics Laboratory, University of Bristol, Royal Fort, Tyndall Avenue, Bristol, BS8 1TL, United Kingdom*

Here we study model dispersions of nanoparticles (radius 55 nm) under confinement by wrinkled surfaces. Confinement is known to have a dramatic effect on the type of stable crystalline structures. High density states of micron-sized particles between two smooth parallel plates display a rich variety of crystals, as found in experiments[12,13] and in simulations of hard sphere model systems.[22,23] Even stronger spatial confinement is provided by cylindrical pores[24–26] or inside grooves on a planar substrate,[20] where wire-like colloidal arrangements are formed. Here we find that highly ordered one-dimensional structures of nanoparticles form upon drying of aqueous colloidal dispersions when these are confined between a smooth planar hydrophilic surface and a wrinkled elastomer. The wavelength of the wrinkles determines the spacing between the (parallel) linear colloidal assemblies. The particle density of the structures can be tuned by varying the particle volume fraction in the initial suspension. A rich variety of ordered structures is observed. We demonstrate that this originates primarily from packing effects of the confined particles by comparing to results from our Monte Carlo computer simulations of the hard sphere model.

The particles were synthesized by emulsion polymerization of styrene with acrylic acid (5.2 mol% relative to styrene) as the comonomer, sodium dodecylsulfate as the emulsifier, and potassium persulfate as the initiator. They possessed an average radius $R = 55$ nm (as determined from dynamic light scattering) with narrow size distribution. The polydispersity index, given as the weight-average diameter divided by the number-average diameter, was only 1.02 (determined by analytic disk centrifugation). The zeta potential of the particles was -55 ± 5 mV, indicating a well-stabilized suspension.

Wrinkled substrates (stamps) were created by stretching a silicon elastomer, poly(dimethyl siloxane) (PDMS), exposing it to an oxygen plasma in order to convert the surface to silica, and subsequent relaxation of the specimen. Stable wrinkles with one dominant wavelength were obtained. Both the wavelength and the amplitude could be controlled *via* the plasma dose applied.[27] In detail, the PDMS elastomer was prepared by mixing Sylgard 184 (purchased from Dow Corning, USA) with a 10 : 1 ratio by mass of pre-polymer to curing agent. The mixture was stirred and filled in a carefully cleaned, plain glass dish. After 24 h at room temperature and baking at 60 °C for 2 h, the cross linked PDMS was cut into 30 × 6 mm stripes. These were stretched in a customer-made apparatus to a linear strain of $\varepsilon = 0.25$. The stretched substrates were exposed for 500 s to an oxygen-plasma at 0.2 mbar using a plasma etcher operating at 0.1 kW (flecto10, Plasma Technology, Germany) to convert the topmost layer to silica. After cooling, the strain was slowly released from the specimen and stable uniform wrinkles were obtained. The glass slides were cleaned using standard RCA-1, performed with a 1 : 1 : 5 solution of $NH_4OH + H_2O_2 + H_2O$ at 75 °C.

This treatment results in the formation of a thin hydrophilic silicon dioxide layer on the glass surface providing appropriate wettability.

After rinsing in water and blow-drying with nitrogen, a drop of nanoparticle suspension (10 μl) was placed onto a glass slide. Immediately after spreading, the wrinkled substrate was placed onto the drop without applying external pressure. After 12 h of drying, the wrinkled PDMS stamp was removed carefully and both surfaces were dried under vacuum. When illuminated with white light, iridescent colors could be observed on the elastomer stamp. This effect is due to interference of the incident light with the periodic substrate. Very similar interference colors[28] appeared also on the glass substrate. Fig. 1a and b display photographs of this effect for two different samples. Scanning electron microscopy (SEM) revealed that the smooth glass substrate was macroscopically covered by parallel prismatic ridges of nanoparticles, see Fig. 1c. These structures remained stable after thorough rinsing in water. The ridges possessed the same spacing as the wrinkles on the stamp, which explains the origin of the iridescent colors. However, besides this structuring on the micron scale, the nanoparticles ordered in crystal-like structures on the particle scale, see the inset of Fig. 1c. SEM images of the wrinkled PDMS stamps showed no appearance of nanoparticles, indicating that the particles stick to the glass surface. Consistent with this, the aqueous suspension of nanoparticles preferentially wets the clean glass surface. It is known that appropriate wetting of wrinkles is essential for colloidal assembly, as shown in ref. 29 and 30.

In order to test whether confinement plays a dominant role in the structuring process, we wish to compare to high-density equilibrium states of a minimal model. We consider hard spheres of radius R confined between one smooth planar hard wall at $z = 0$ and one sinusoidal hard wall at $z = L_z + a[\sin(2\pi x/\lambda)-1]$. Here z is the coordinate across the slit, L_z is a measure of the distance of the two walls, a is the amplitude of the sinusoidal corrugation, λ is its wavelength, and x is the lateral coordinate perpendicular to the wrinkles. Any direct interactions between the two walls are omitted. Fig. 2 displays an illustration of the model, for which we carried out Monte Carlo computer simulations for a wide range of different values of particle concentrations and for several values of the amplitude a. The wavelength was fixed to the experimentally determined value of $\lambda = 17.38R$. Periodic boundary conditions were applied in the x and y (along the wrinkles) directions, and the box size in the x-direction was chosen as 4λ. We kept the number of particles $N = 800$ constant, as well as the lateral area $L_x \times L_y = const.$ The length L_z was allowed to fluctuate, such that the z component of the pressure, P_z, was kept constant at a finite, but large value of $P_z = 1.875 k_B T/R^3$, where k_B is the Boltzmann constant and T is absolute temperature. The simulations were started at a value of $L_z \gg a$, such that the system was in a disordered, low-density fluid state. Then the system was equilibrated for a total of 10^7 MC steps per particle. The linear density $\rho = RN\lambda/(L_yL_x)$ was kept constant throughout the compression procedure. Clearly, all effects due to capillary bridges of the drying solvent as well as due to charges and van der Waals forces are neglected.

The type of experimentally observed particle assemblage could be controlled by varying the volume fraction ϕ of particles in the initial dispersion. Fig. 3 (left column) displays a sequence of SEM pictures of structures for a stamp with $\lambda = 956$ nm. The difference between minima and maxima (*i.e.* twice the value of the amplitude) of the substrate was 148 nm, as obtained by analyzing atomic force microscopy (AFM) height profiles. At low density ($\phi = 0.002$, Fig. 3a) we found parallel lines of particles in single file. For increasing density ($\phi = 0.004$, Fig. 3b) we found two lines of particles, a pyramidal prism with two particles in the base and one on top ($\phi = 0.007$, Fig. 3c), a pyramidal prism with three particles in the base and two on top (Fig. 3d), and finally a larger pyramidal prism with four particles in the base ($\phi = 0.014$, Fig. 3e). The only prismatic structures reported in the literature are, to the best of our knowledge, those of much larger, micron-sized, spheres.[15] By counting particles we obtained the linear density ρ of particles per unit length (taken as the particle radius R) of the particle arrays. We compare to simulation results that we have obtained for the same values of ρ. The resulting hard sphere structures are shown from the top (middle column in Fig. 3) and along the channels (right column). All structures agree very well with their experimental counterparts, even reproducing accurately the types of defects that occur. We expect the defects to originate (i) partly from the kinetics of the compression process, but

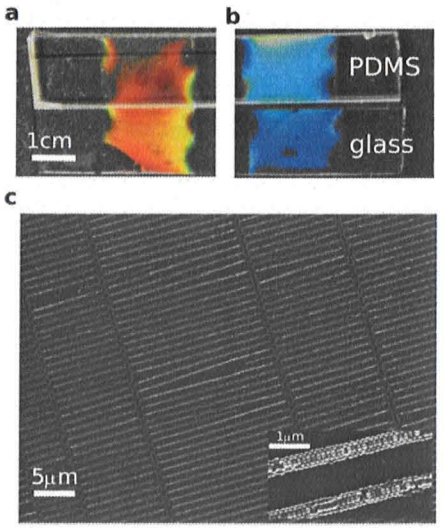

Fig. 1 Digital camera pictures (a and b) of wrinkled PDMS stamps (above) and decorated glass substrates (below). The different iridescent colors in (a) and (b) stem from periodically structured features of the surface with different wavelengths (956 nm and 765 nm, respectively). The SEM image in (c) shows prismatic structures assembled on the glass substrate, with spacing between prisms that matches the wavelength of the wrinkles. Perpendicular bridges of particles originate from cracks on the stamp on a larger length scale. The inset shows a magnified section of the main picture.

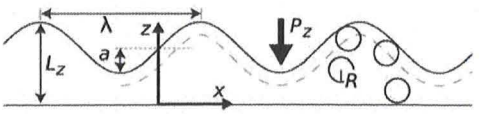

Fig. 2 An illustration of the theoretical model of hard spheres with radius R confined between a (lower) smooth hard wall and an (upper) hard wall with sinusoidal shape of wavelength λ and amplitude a. The (maximal) distance between both walls is denoted by L_z. The pressure P_z acts on the top wall; the lower wall is kept fixed. The dashed lines indicate the depletion zones that are inaccessible to the particle centers, due to interactions of the particles with the walls. z is the coordinate across the slit; x and y are the lateral coordinates; y (not shown) is perpendicular to the image plane.

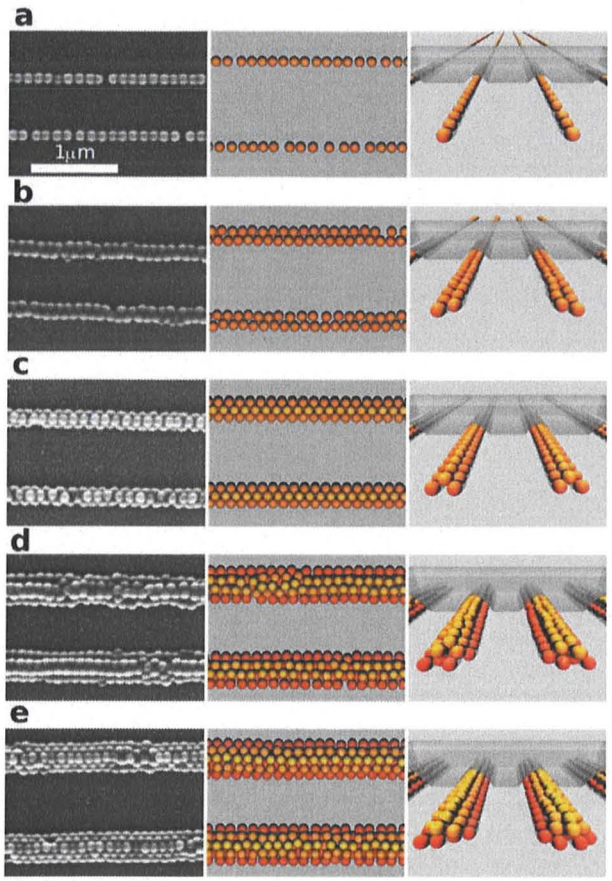

Fig. 3 Sequence of structures found experimentally with SEM (left column) and in simulations, shown from the top (middle column) and along the channels (right column). The concentration increases from (a) to (e), leading to structures that range from single-file wires to prisms with triangular cross section. The transparent grey shape represents the sinusoidal wall and is shown only partially for clarity.

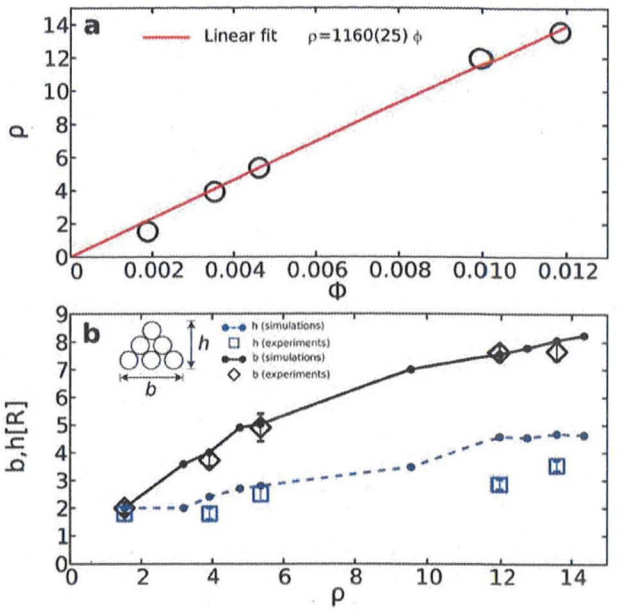

Fig. 4 (a) Experimental results (symbols) for the dependence of the linear density ρ of assembled particles on the initial volume fraction ϕ of particles in the dispersion. The line is a linear fit to the data. (b) Variation of the geometry of the colloidal structures with their density ρ. Shown are the height h and base b of the prism structures (see inset for a cross section) in units of particle radius R as obtained in simulations (filled symbols joined by lines to guide the eye) and AFM measurements (open symbols with error bars).

also (ii) from intrinsic disorder that is of thermal, entropic origin. The structures with more than two lines of particles possess the same triangular, prism-like cross section as were found experimentally. The simulation results were obtained by choosing the amplitude $a = 3.6R$, significantly larger than half of the experimental value for the free stamp, 74 nm $= 1.35R$. However, in our model we allow for overlap of both walls, such that $L_z < 2a$. We take the resulting pore shapes (*cf.* right column of Fig. 3) as a simple model for the real channels, which we expect to be influenced by deformation of the wrinkles when in contact with a hard substrate.[27]

Remarkably, the experimentally observed variation of ρ with the initial packing fraction ϕ is nearly linear, see Fig. 4a. This allows to tune ρ, and hence the type of ordered structure, accurately by simple variation of ϕ. We measured the relevant geometrical dimensions of the structures, namely the base b and height h (see the inset of Fig. 4 b for an illustration). Values for b were determined by image analysis of SEM pictures; those for h were determined from height profiles measured by AFM. In the computer simulations the results for b and h were obtained by measuring density profiles in the direction perpendicular to the prisms and in the z -direction, respectively. We find quantitative agreement of the results from the two approaches for the variation of b with ρ, see Fig. 4b. The values for the height h as a function of ρ as determined in experiment are consistently smaller than those found in simulations. Part of this deviation could be due to shrinking of the particles upon drying; the particle diameter as measured by AFM is 10% smaller than the hydrodynamic value. Nevertheless, the general agreement is very satisfactory, in particular given the simplicity of the model.

Even more complex structures were formed, when the suspension was confined between *two* wrinkled stamps, with channel directions at a right angle. The resulting grid-like structure of particles possessed completely different, strongly interconnected topology, see Fig. 5a for an SEM image. Correspondingly, in simulations we confined the hard sphere model between two sinusoidal walls with crossed orientations, and hence replaced the lower (smooth) wall by $z = a[\sin(2\pi y/\lambda) + 1]$ with $L_x = L_y = 4\lambda$ and chose $N = 2780$ in order to match roughly the experimental situation. The resulting structure, see Fig. 5b, reproduced very well the features of the experimental result. Moreover, crossing two stamps at an angle of 45° creates a chiral grid with ellipsoidal holes (Fig. 5c) that could again be reproduced in simulation (Fig. 5d) by counter-rotating two sinusoidal walls (initially with wave vector in the x-direction) by ±22.5° and choosing $L_x = 2\lambda/\sin(22.5°)$, $L_y = 2\lambda/\cos(22.5°)$ and $N = 1537$.

We proposed a versatile method for hierarchical nanoparticle structuring that allows for easy control of spacing and density of particle arrays on a smooth planar hydrophilic substrate. Macroscopic coverage can be obtained. As the assembly is driven by packing effects, the details of the chemistry play only a minor role: we could obtain very similar structuring using, instead of polystyrene, other organic and gold nanoparticles. Linear

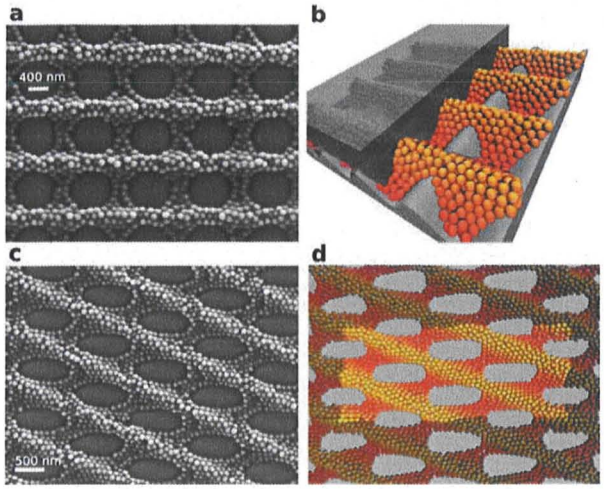

Fig. 5 (a) SEM image of a dried colloidal suspension that was confined between two crossed wrinkled stamps. (b) Perspective view of a simulation configuration of hard spheres confined between two sinusoidal walls with crossed orientations. Half of the upper wall is cut away for clarity. (c) As in (a) but for two stamps that were crossed by an angle of 45°. (d) Top view of the simulation configuration corresponding to (c). Particles that belong to periodic images are shaded grey. Note the chiral nature of the structure in (c) and (d); this cannot be transformed by rotations and translations only into its chiral partner with crossing angle of −45°).

structures of the latter are well suited for optical applications, such as surface enhanced Raman spectroscopy.[31] It would be interesting to investigate the interplay of drying and adhesion under confinement, and the role of dispersion forces in the assembly process in future work. We leave a systematic investigation of the dependence of the type of colloidal structures on the wavelength and amplitude of the wrinkles on the stamp to future work.

Acknowledgements

We thank Moritz Tebbe for helpful assistance in carrying out some of the experimental work and Mark Dennis and Paddy Royall for useful comments on the manuscript. A.S. thanks the German Science Foundation (DFG) for support within the SFB481. A.Fo. and M.S. thank the DFG for support *via* SFB840/A3, A.Fe. and A.W. *via* SFB840/B5.

References

1 Z. Sun and B. Yang, *Nanoscale Res. Lett.*, 2006, **1**, 46–56.
2 S. J. Koh, *Nanoscale Res. Lett.*, 2007, **2**, 519–545.
3 S. Mitragotri and J. Lahann, *Nat. Mater.*, 2008, **8**, 15–23.
4 J. A. Schuller, E. S. Barnard, W. Cai, Y. C. Jun, J. S. White and M. L. Brongersma, *Nat. Mater.*, 2010, **9**, 193–204.
5 H. A. Atwater and A. Polman, *Nat. Mater.*, 2010, **9**, 205–213.
6 Y. Xia, Y. Yin, Y. Lu and J. McLellan, *Adv. Funct. Mater.*, 2003, **13**, 907–918.
7 K. Chen, X. Jiang, L. Kimerling and P. T. Hammond, *Langmuir*, 2000, **16**, 7825–7834.
8 P. Maury, M. Escalante, D. Reinhoudt and J. Huskens, *Adv. Mater.*, 2005, **17**, 2718–2723.
9 J. Aizenberg, P. Braun and P. Wiltzius, *Phys. Rev. Lett.*, 2000, **84**, 2997–3000.
10 A. van Blaaderen, R. Ruel and P. Wiltzius, *Nature*, 1997, **385**, 321–324.
11 J. Hoogenboom, C. Retif, E. de Bres, M. de Boer, A. van Langen-Suurling, J. Romijn and A. van Blaaderen, *Nano Lett.*, 2004, **4**, 205–208.
12 Pa. Pieranski, L. Strzelecki and B. Pansu, *Phys. Rev. Lett.*, 1983, **50**, 900–903.
13 S. Neser, C. Bechinger, T. Palberg and P. Leiderer, *Phys. Rev. Lett.*, 1997, **79**, 2348–2351.
14 Y. Masuda, T. Itoh, M. Itoh and K. Koumoto, *Langmuir*, 2004, **20**, 5588–5592.
15 T. Mitsui, Y. Wakayama, T. Onodera, Y. Takaya and H. Oikawa, *Nano Lett.*, 2008, **8**, 853–858.
16 Y. Xia and G. Whitesides, *Annu. Rev. Mater. Sci.*, 1998, **28**, 153–184.
17 E. Kim, Y. Xia and G. M. Whitesides, *Adv. Mater.*, 1996, **8**, 245–247.
18 A. Hung and S. Stupp, *Nano Lett.*, 2007, **7**, 1165–1171.
19 N. Bowden, S. Brittain, A. G. Evans, J. W. Hutchinson and G. M. Whitesides, *Nature*, 1998, **393**, 146–149.
20 C. Lu, H. Möhwald and A. Fery, *Soft Matter*, 2007, **3**, 1530–1536.
21 J. Genzer and J. Groenewold, *Soft Matter*, 2006, **2**, 310–323.
22 M. Schmidt and H. Löwen, *Phys. Rev. Lett.*, 1996, **76**, 4552–4556.
23 A. Fortini and M. Dijkstra, *J. Phys.: Condens. Matter*, 2006, **18**, L371–L378.
24 G. T. Pickett, M. Gross and H. Okuyama, *Phys. Rev. Lett.*, 2000, **85**, 3652–3655.
25 F. Li, X. Badel, J. Linnros and J. B. Wiley, *J. Am. Chem. Soc.*, 2005, **127**, 3268–3269.
26 M. Tymczenko, L. F. Marsal, T. Trifonov, I. Rodriguez, F. Ramiro-Manzano, J. Pallares, A. Rodriguez, R. Alcubilla and F. Meseguer, *Adv. Mater.*, 2008, **20**, 2315–2318.
27 M. Pretzl, A. Schweikart, C. Hanske, A. Chiche, U. Zettl, A. Horn, A. Böker and A. Fery, *Langmuir*, 2008, **24**, 12748–12753.
28 See, *e.g.*, O. L. J. Pursiainen, J. J. Baumberg, H. Winkler, B. Viel, P. Spahn and T. Ruhl, *Opt. Express*, 2007, **15**, 9553–9561 and references therein.
29 Y. J. Chung, J. P. Youngblood and C. M. Stafford, *Soft Matter*, 2007, **3**, 1163.
30 T. Ohzono, H. Monobe, H. Shiokawa, M. Fujiwara and Y. Shimizu, *Soft Matter*, 2009, **5**, 4658.
31 N. Pazoz-Pérez, W. Ni, A. Schweikart, R. A. Alvarez-Puebla, A. Fery and L. M. Liz-Marzán, *Chem. Sci.*, 2010, **1**, 174–178.